

Geometric phase gates based on stimulated Raman adiabatic passage in tripod systems

Ditte Møller,* Lars Bojer Madsen, and Klaus Mølmer

*Lundbeck Foundation Theoretical Center for Quantum System Research,
Department of Physics and Astronomy, University of Aarhus, DK-8000, Denmark.*

(Dated: September 19, 2018)

We consider stimulated Raman adiabatic passage (STIRAP) processes in tripod systems and show how to generate purely geometric phase changes of the quantum states involved. The geometric phases are controlled by three laser fields where pulse shapes, relative field strength and phases can be controlled. We present a robust set of universal gates for quantum computing based on these geometric phases: a one-qubit phase gate, a Hadamard gate and a two-qubit phase gate.

PACS numbers: 03.67.Lx,03.65.Vf,42.50.-p

I. INTRODUCTION

With the growing interest in quantum computation and information the search for efficient and robust quantum gates has become increasingly important. Deutsch presented in 1989 a three qubit quantum gate and showed that this gate together with arbitrary one-qubit rotations are sufficient to create any quantum network [1]. Such a set of gates are called universal for quantum computation. Since then many sets of gates were proven to be universal [2] - one of them consisting of a one-qubit phase gate (S), a one-qubit Hadamard gate (H), and a two-qubit controlled phase gate (CS). Explicitly in the one- and two-qubit bases ($\{|0\rangle, |1\rangle\}$, $\{|00\rangle, |01\rangle, |10\rangle, |11\rangle\}$) the form of these gates are

$$S = \begin{bmatrix} 1 & 0 \\ 0 & e^{i\phi_1} \end{bmatrix}, \quad H = \frac{1}{\sqrt{2}} \begin{bmatrix} 1 & 1 \\ 1 & -1 \end{bmatrix}, \quad (1)$$

$$CS = \frac{1}{\sqrt{2}} \begin{bmatrix} 1 & 0 & 0 & 0 \\ 0 & 1 & 0 & 0 \\ 0 & 0 & 1 & 0 \\ 0 & 0 & 0 & e^{i\phi_2} \end{bmatrix}.$$

The purpose of the present work is to show that all these gates can be implemented using only gates based on adiabatic evolution using stimulated Raman adiabatic passage (STIRAP) and leading to geometric phases. A quantum system which starts out in the n 'th eigenstate of a Hamiltonian that changes adiabatically in time will according to the adiabatic theorem [3] remain in the n 'th eigenstate but may acquire a phase. In 1984 Berry showed that besides a dynamical part $\theta_n = -\int \omega_n(t)dt$ associated with the eigenfrequency $\omega_n = E_n/\hbar$ the state also acquires a geometric phase, γ_n [4]

$$\Psi(0) = \psi_n(0) \rightarrow \Psi(t) = \exp[i(\theta_n + \gamma_n)]\psi_n(t). \quad (2)$$

The geometric part depends on the geometric properties of the parameter space of the Hamiltonian and Berry

showed how to calculate γ_n when the eigenstate is known and the system is non-degenerate [4]. Berry's phase was generalized to degenerate systems by Wilczek and Zee [5] and to non-adiabatic evolution of the system by Aharonov and Anandan [6]. Quantum computation relying on these geometric quantum phases is called holonomic quantum computation [7] and is expected to be particularly robust against noise. Previously, proposals for holonomic quantum computation were presented for nuclear magnetic resonance [8], neutral atoms [9] and trapped ions [10].

Control of the geometric phases requires an adiabatic evolution and preferably an eigenstate with a zero-valued eigenenergy in order to avoid the build-up of an additional dynamic phase as the system evolves. A well-described adiabatic process is STIRAP where population is transferred from one quantum state to another in a three-level lambda-system when subject to two different laser pulses ordered in a counterintuitive time-sequence [11]. The STIRAP process was shown to be very efficient and robust theoretically as well as experimentally [11, 12, 13, 14, 15, 16, 17, 18]. Geometric phases accumulated during a STIRAP process were previously investigated for tripod systems [19] and used for single-qubit rotations [20], entanglement between atoms in a cavity [21] and holonomic quantum computation with trapped ions [10]. In [22] these phases were considered for an open quantum system. In this work, we present an experimental implementable set of universal gates based on geometric phases arising from population transfer in tripod systems and show explicitly how they depend on the experimental parameters.

The paper is organized as follows: Sec. II presents the atomic system under consideration. In Sec. III we present a one-qubit phase gate and in Sec. IV the Hadamard gate. The gates are investigated analytically as well as numerically. In Sec. V we introduce a coupling between the two qubits and present a two-qubit controlled phase gate. In Sec. VI we discuss the robustness and conclude.

*Electronic address: dittem@phys.au.dk

II. TRIPOD SYSTEM

We consider two atoms (ions or neutrals) with a tripod level structure as shown in Fig. 1. The three lower states ($|0\rangle, |1\rangle$ and $|2\rangle$) are long-lived and coupled to the upper state $|e\rangle$ by application of three laser fields with Rabi frequencies $\Omega_0, \Omega_1, \Omega_2$, respectively. In practice the lower states can be ground Zeeman- or hyperfine-sublevels, and $|e\rangle$ is an electronically excited state or excited state manifold. We assume the laser fields are on two-photon resonance and denote the one-photon detuning by Δ . We use STIRAP processes to transfer population among the three lower states and the excited state $|e\rangle$ is therefore never populated during the process which ensures that no loss occurs due to spontaneous emission. We consider $\{|0\rangle, |1\rangle\}$ as our qubit-states. In the follow-

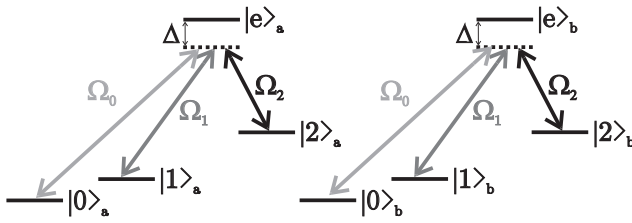


FIG. 1: Two atomic four-level tripod systems with three laser fields applied with Rabi frequencies $\Omega_0, \Omega_1, \Omega_2$. The one-photon detuning is denoted by Δ , and the subscripts a and b refer to two different atoms.

ing we implement the universal set of quantum gates (1) using geometric phases acquired by transferring population adiabatically with STIRAP-processes.

III. ONE-QUBIT PHASE GATE

We first consider how to use STIRAP to perform a simple one-qubit phase gate: $|j\rangle \rightarrow e^{i\phi_j}|j\rangle$ where $|j\rangle$ is either of the two qubit states $|0\rangle$ and $|1\rangle$. For this purpose we use a single STIRAP process to transfer the population from $|j\rangle$ to $|2\rangle$ and another to transfer the population back to $|j\rangle$ again. During this process $|j\rangle$ gains a geometric phase. The total pulse sequence is shown in Fig. 2. To solve the time evolution during these two STIRAP sequences we consider the Hamiltonian for the $\{|j\rangle, |e\rangle, |2\rangle\}$ lambda system in the rotating wave approximation (RWA), when we assume two-photon resonance between $|j\rangle$ and $|2\rangle$ (see Fig. 1)

$$H(t) = \frac{\hbar}{2} \begin{bmatrix} 0 & \Omega_j(t) & 0 \\ \Omega_j^*(t) & 2\Delta & \Omega_2(t) \\ 0 & \Omega_2^*(t) & 0 \end{bmatrix}. \quad (3)$$

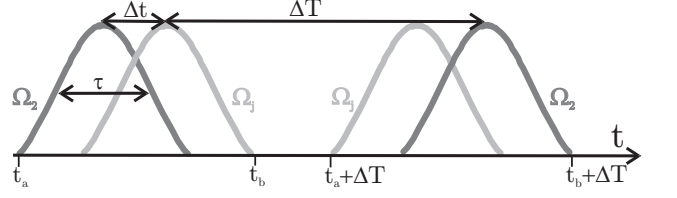


FIG. 2: Pulse sequence transferring population from $|j\rangle$ to $|2\rangle$ and back to $|j\rangle$ again. The FWHM of each of the four pulses is τ (see Eq. (13)), ΔT is the delay between the two sequences and Δt the delay between two pulses within one sequence.

We parameterize the complex Rabi frequencies as

$$\Omega_j(t) = \sin \theta(t) \sqrt{|\Omega_j(t)|^2 + |\Omega_2(t)|^2}, \quad (4)$$

$$\Omega_2(t) = \cos \theta(t) \sqrt{|\Omega_j(t)|^2 + |\Omega_2(t)|^2} e^{i\varphi(t)}, \quad (5)$$

and diagonalize (3) to obtain the energy eigenvalues

$$\omega^\pm = \Delta \pm \sqrt{\Delta^2 + \Omega_j^2 + \Omega_2^2}, \quad \omega^D = 0, \quad (6)$$

with the non-absorbing zero-valued dark state ($\omega^D = 0$) given by

$$|D(t)\rangle = \cos \theta(t) |j\rangle - \sin \theta(t) e^{i\varphi(t)} |2\rangle. \quad (7)$$

Now we assume that this state is the initial state $|\psi(-\infty)\rangle = |D(-\infty)\rangle$ at time $t = -\infty$ before the pulses and that we vary the real amplitudes of $\Omega_j(t)$ and $\Omega_2(t)$ and the phase $\varphi(t)$ of $\Omega_2(t)$ in an adiabatic way such that all population stays in $|D(t)\rangle$. During this evolution the $|D(t)\rangle$ -state will pick up a phase which is purely geometric because the state has zero energy eigenvalue. The phase will depend on the evolution of the parameters θ and φ and we define these as a vector, $\vec{R} = (\theta(t), \varphi(t))$, in parameter-space of the Hamiltonian. Then the acquired Berry phase is exactly the integral

$$\gamma_{n_1} = i \int_{\vec{R}_i}^{\vec{R}_f} \langle D | \nabla_{\vec{R}} | D \rangle \cdot d\vec{R} = - \int_{\varphi(t_i)}^{\varphi(t_f)} \sin^2 \theta(t) d\varphi(t), \quad (8)$$

where $\sin^2 \theta$ is found from Eq. (4)

$$\sin^2 \theta(t) = \frac{\Omega_j^2(t)}{|\Omega_j(t)|^2 + |\Omega_2(t)|^2}. \quad (9)$$

In the pulse sequence of Fig. 2 we assume that all four pulses are described by the common function $\Omega(t)$. In addition to $\Omega(t)$, the Rabi frequency $\Omega_2(t)$ is defined by the phase $\varphi(t)$ (see Eq. (5)). The instants of time t_a and t_b in Fig. 2 are defined such that $\sin^2 \theta(t) \approx 0$ for $t < t_a \vee t > t_b + \Delta T$ and $\sin^2 \theta(t) \approx 1$ for $t_b < t < t_a + \Delta T$.

With these definitions we obtain from Eq. (8) and (9)

$$\begin{aligned} \gamma_{n_1} = & - \int_{\varphi(t_a)}^{\varphi(t_b)} \frac{\Omega^2(t)}{\Omega^2(t) + \Omega^2(t + \Delta t)} d\varphi \quad (10) \\ & - \int_{\varphi(t_b)}^{\varphi(t_a + \Delta T)} 1 d\varphi \\ & - \int_{\varphi(t_a + \Delta T)}^{\varphi(t_b + \Delta T)} \frac{\Omega^2(t + \Delta t - \Delta T)}{\Omega^2(t + \Delta t - \Delta T) + \Omega^2(t - \Delta T)} d\varphi. \end{aligned}$$

Substituting $t' = t - \Delta T$ in the last integral and assuming that φ is a monotonic function we obtain

$$\begin{aligned} \gamma_{n_1} = & - \int_{t_a}^{t_b} \frac{\Omega^2(t)}{\Omega^2(t) + \Omega^2(t + \Delta t)} \cdot \frac{d\varphi}{dt} dt \quad (11) \\ & - \int_{t_b}^{t_a + \Delta T} \frac{d\varphi}{dt} dt \\ & - \int_{t_a}^{t_b} \frac{\Omega^2(t' + \Delta t)}{\Omega^2(t' + \Delta t) + \Omega^2(t')} \cdot \frac{d\varphi}{dt} dt' \\ = & - \int_{t_a}^{t_a + \Delta T} \frac{d\varphi}{dt} dt = \varphi(t_a) - \varphi(t_a + \Delta T). \end{aligned}$$

The geometric phase thus only depends on the laser field phases and requires control of ΔT , the fraction $\frac{\Omega_j(t)}{\Omega_2(t)}$ and similarity of the four pulses. All these quantities are routinely controlled to high precision in present-day laboratories. After the evolution the final state is

$$|\psi_f(t)\rangle = e^{i\gamma_{n_1}} |j\rangle. \quad (12)$$

The population and the phases of the three states $|j\rangle$, $|e\rangle$ and $|2\rangle$ can be found numerically by solving the time-dependent Schrödinger equation. In addition the phases can be calculated analytically as described above (Eq. (11) and (12)). In Fig. 3 we show the population of the states as well as the evolution of their phases when we assume $\varphi = t/T_0 \Rightarrow \gamma_{n_1} = -\Delta T/T_0$ and use \sin^2 -pulses with same amplitude

$$\Omega(t) = \begin{cases} \Omega_{\max} \sin^2(\frac{\pi t}{2\tau}) & \text{if } 0 < t < 2\tau \\ 0 & \text{otherwise} \end{cases}. \quad (13)$$

The factor of 2 in the pulse assures that τ corresponds to the FWHM. The populations are shown in the upper panel of Fig. 3. Initially all population is in the $|j\rangle$ -state (full curve). During the first STIRAP-process the population is transferred from $|j\rangle$ to $|2\rangle$ (dotted curve) while the second STIRAP-process transfers the population back to $|j\rangle$. The electronic excited $|e\rangle$ -state (dashed curve) is never populated and hence no loss of population occurs due to spontaneous emission from $|e\rangle$. The evolution of the phases is shown in the lower panel of Fig. 3. The full curve shows the phase of $|j\rangle$. This phase is the geometric phase $\phi_j = \gamma_{n_1}$. The phase ϕ_j remains zero until the first set of STIRAP pulses arrive (t_a in Fig. 2); it then accumulates a phase until the second pair of pulses has passed ($t_b + \Delta T$ in

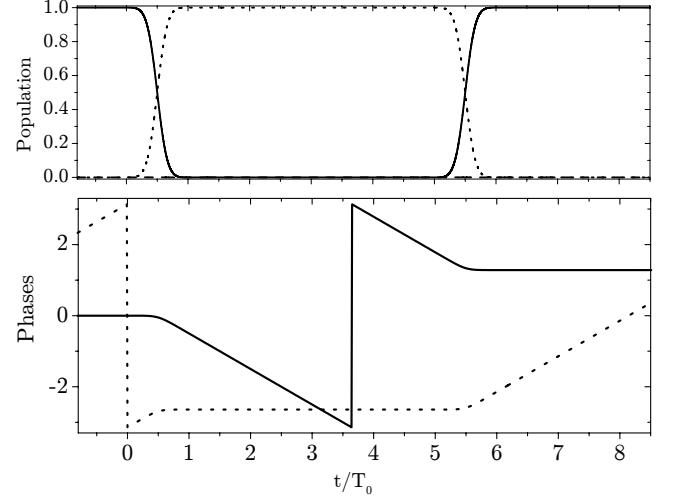


FIG. 3: The upper panel shows the evolution of the population of states $|j\rangle$ (full), $|e\rangle$ (dashed), and $|2\rangle$ (dotted). The lower panel shows the evolution of the phases, ϕ_j of state $|j\rangle$ (full) and ϕ_2 of state $|2\rangle$ (dotted). Numerical and analytical results cannot be distinguished on the scale of the figure. The calculations were made with \sin^2 -pulses (13), $\varphi = t/T_0$ and parameters: $\Omega_{\max,j}/2\pi = \Omega_{\max,2}/2\pi = 100/T_0$, $\Delta t/T_0 = 1$, $\tau/T_0 = 1$, $\Delta T/T_0 = 5$.

Fig. 2). The total acquired phase is as shown in Eq. (11), $\gamma_{n_1} = \varphi(t_a) - \varphi(t_a + \Delta T) = -\Delta T/T_0$. The phase of the $|2\rangle$ -state (dotted curve) contains not only the geometric phase γ_{n_1} but also the additional $\varphi(t) - \pi$ (See Eq. 7) yielding a total phase $\phi_2 = \gamma_{n_1} + \varphi(t) - \pi$. The $|2\rangle$ -state therefore accumulates a phase before the first and after the second STIRAP process -but not in between where γ_{n_1} and $\varphi(t)$ cancel each other. In the time-windows where the states in question are populated the direct numerical solution of the time-dependent Schrödinger equation gives results for the phases in agreement with the above analytical results.

IV. HADAMARD GATE

To implement a Hadamard gate we use three laser fields with Rabi frequencies Ω_0 , Ω_1 and Ω_2 (See Fig. 1). We apply Ω_0 and Ω_1 in a constant ratio $\tan \theta_{01} = \frac{|\Omega_0|}{|\Omega_1|}$ with phase difference ϕ_{01} and assume two-photon resonance. In this case the dressed states of the system are

a single dark ($|D_H\rangle$) and two bright states ($|+\rangle, |-\rangle$)

$$\begin{aligned} |D_H\rangle &= \cos\theta_{01}(t)|0\rangle - \sin\theta_{01}(t)e^{i\phi_{01}}|1\rangle, \\ |+\rangle &= \frac{1}{\sqrt{2}}(\sin\delta(\sin\theta_{01}(t)|0\rangle + \cos\theta_{01}(t)e^{i\phi_{01}}|1\rangle) \\ &\quad + \cos\delta|e\rangle), \\ |-\rangle &= \frac{1}{\sqrt{2}}(\cos\delta(\sin\theta_{01}(t)|0\rangle + \cos\theta_{01}(t)e^{i\phi_{01}}|1\rangle) \\ &\quad - \sin\delta|e\rangle), \end{aligned} \quad (14)$$

with eigenvalues $\omega_{D_H} = 0$, $\omega_{\pm} = \Delta \pm \sqrt{\Delta^2 + \Omega_0^2 + \Omega_1^2}$ and δ defined by $\tan\delta = \sqrt{\frac{-\omega_-}{\omega_+}}$. To ensure that no population is transferred to the $|e\rangle$ -state we choose as our initial state

$$\begin{aligned} |\psi_i\rangle &= a|D_H\rangle + \sqrt{2}b(\sin\delta|+\rangle + \cos\delta|-\rangle) \\ &= a|D_H\rangle + b(\sin\theta_{01}|0\rangle + \cos\theta_{01}e^{i\phi_{01}}|1\rangle) \\ &= a|D_H\rangle + b|B\rangle, \end{aligned} \quad (15)$$

where a, b are normalization constants and $|B\rangle = \sin\theta_{01}|0\rangle + \cos\theta_{01}e^{i\phi_{01}}|1\rangle$ is the bright part of $|\psi_i\rangle$. We now use the same pulse sequence as in the case of the one-qubit phase gate (Fig. 2) but with both Ω_0 and Ω_1 applied. The dark state $|D_H\rangle$ does not couple to $|2\rangle$ and is therefore unaffected by the pulses, while the bright state $|B\rangle$ does couple and is therefore transferred to $|2\rangle$ and back again acquiring a geometric phase. In this sense the dynamics is similar to the one-qubit case and accordingly $|B\rangle \rightarrow e^{i\gamma_{n_H}}|B\rangle$ with $\gamma_{n_H} = -\int \sin^2\theta_H d\varphi_H$. The geometric phase γ_{n_H} is controlled by $\tan\theta_H = \frac{\sqrt{|\Omega_0|^2 + |\Omega_1|^2}}{|\Omega_2|}$ and φ_H , which is the phase difference between Ω_0 and Ω_2 . After the pulses the system then ends up in

$$\begin{aligned} |\psi_f\rangle &= a|D_H\rangle + be^{i\gamma_{n_H}}|B\rangle \\ &= a|D_H\rangle + be^{i\gamma_{n_H}}(\sin\theta_{01}|0\rangle + \cos\theta_{01}e^{i\phi_{01}}|1\rangle). \end{aligned} \quad (16)$$

To implement the Hadamard gate we control the Rabi frequencies to obtain $\Omega_{\max,2} = \sqrt{\Omega_{\max,0}^2 + \Omega_{\max,1}^2}$ and $\Omega_0 = -(\sqrt{2} - 1)\Omega_1$. This latter relation leads to $\theta_{01} = \frac{\pi}{8}$ and $\phi_{01} = \pi$. We control the pulse sequence such that $\gamma_{n_H} = -\pi$ and with these parameters we find from (14), (15) and (16)

$$\begin{aligned} |\psi_i\rangle &= (a \cos \frac{\pi}{8} + b \sin \frac{\pi}{8})|0\rangle + (a \sin \frac{\pi}{8} - b \cos \frac{\pi}{8})|1\rangle \quad (17) \\ |\psi_f\rangle &= (a \cos \frac{\pi}{8} - b \sin \frac{\pi}{8})|0\rangle + (a \sin \frac{\pi}{8} + b \cos \frac{\pi}{8})|1\rangle \end{aligned}$$

Now the initial condition $|\psi_i\rangle = |0\rangle$ corresponds to $(a, b) = (\cos(\frac{\pi}{8}), \sin(\frac{\pi}{8}))$ yielding a final state $|\psi_f\rangle = \frac{1}{\sqrt{2}}(|0\rangle + |1\rangle)$, while $|\psi_i\rangle = |1\rangle$ corresponds to $(a, b) =$

$(\sin(\frac{\pi}{8}), -\cos(\frac{\pi}{8}))$ yielding a final state $|\psi_f\rangle = \frac{1}{\sqrt{2}}(|0\rangle - |1\rangle)$. With this degree of control we therefore produce a Hadamard gate with certainty. This gate combined with the one-qubit phase gate can generate arbitrary qubit rotations and the gate is robust as it depends on controllable parameters such as the pulse shapes, the ratio of Rabi frequencies, the delay between the two sequences and the phases of the laser fields.

V. TWO-QUBIT PHASE GATE

To create a two-qubit phase gate a coupling between the two qubits is necessary. We consider a coupling $E|22\rangle\langle 22|$, where E is the coupling strength. In the end of this section, we briefly discuss how such a coupling can be realized. We assume real Rabi frequencies and all laser fields on resonance. If we wish to solve the full system of Fig. 1 analytically it is an advantage to go into the interaction picture with respect to $H_0 = E|22\rangle\langle 22|$. In this picture the system has a six-dimensional null-space yielding six orthonormal dark states, $|D_i\rangle$ ($i = 1, \dots, 6$):

$$\begin{aligned} |D_1\rangle &= |00\rangle, \\ |D_2\rangle &= -\cos\theta_2|10\rangle + \sin\theta_2|20\rangle, \\ |D_3\rangle &= -\cos\theta_2|01\rangle + \sin\theta_2|02\rangle, \\ |D_4\rangle &= \frac{1}{\sqrt{2}}(\sin\theta_2(|1e\rangle - |e1\rangle) + \cos\theta_2(|2e\rangle - |e2\rangle)), \\ |D_5\rangle &= \cos^2\theta_2|11\rangle - \sin\theta_2\cos\theta_2(|12\rangle + |21\rangle) \\ &\quad + \sin^2\theta_2e^{iEt}|22\rangle, \\ |D_6\rangle &= \frac{1}{\sqrt{2}}(-\sin^2\theta_2|11\rangle - \sin\theta_2\cos\theta_2(|12\rangle + |21\rangle) + |ee\rangle \\ &\quad - \cos^2\theta_2e^{iEt}|22\rangle). \end{aligned} \quad (18)$$

In this degenerate case we use the method described by Wilczek and Zee [5] to find the geometric phases. We assume that we start with all population in $|11\rangle$ and that only Ω_2 is applied and write $\psi_I(-\infty) = |D_5(-\infty)\rangle$, where the index I indicates that we are solving the problem in the interaction picture. When we assume an adiabatic evolution the population stays within the null-space and $\psi_I(t)$ can be written as (see also Ref. [19])

$$\psi_I(t) = \sum_b B_b(t)|D_b(t)\rangle. \quad (19)$$

The time evolution is given by the time-dependent Schrödinger equation (dot denotes differentiation with

respect to time)

$$\begin{aligned}\dot{\psi}_I(t) &= \frac{-i}{\hbar}(H(t) - H_0(t))\psi_I(t) = 0 \Rightarrow \\ \sum_b \dot{B}_b(t)D_b(t)\rangle + B_b(t)|\dot{D}_b(t)\rangle &= 0 \Rightarrow \\ \sum_b \dot{B}_b(t)|D_b(t)\rangle &= -\sum_b B_b(t)|\dot{D}_b(t)\rangle.\end{aligned}\quad (20)$$

Here we have used that $(H(t) - H_0(t))|D_b(t)\rangle = 0$ for all dark states. Taking the inner product with $\langle D_c(t)|$ yields

$$\dot{B}_c(t) = -\sum_b B_b(t)\langle D_c(t)|\dot{D}_b(t)\rangle. \quad (21)$$

The only non-zero $\langle D_c(t)|\dot{D}_b(t)\rangle$ -elements are

$$\begin{aligned}\langle D_5(t)|\dot{D}_5(t)\rangle &= iE \sin^4 \theta, \\ \langle D_5(t)|\dot{D}_6(t)\rangle &= \frac{i}{\sqrt{2}}E \cos^2 \theta_2 \sin^2 \theta_2, \\ \langle D_6(t)|\dot{D}_5(t)\rangle &= \frac{i}{\sqrt{2}}E \cos^2 \theta_2 \sin^2 \theta_2, \\ \langle D_6(t)|\dot{D}_6(t)\rangle &= \frac{i}{2}E \cos^4 \theta_2.\end{aligned}\quad (22)$$

The differential equations for the B -coefficients now reduce to

$$\begin{aligned}\dot{B}_1(t) &= 0, \dot{B}_2(t) = 0, \dot{B}_3(t) = 0, \dot{B}_4(t) = 0, \\ \dot{B}_5(t) &= -iE \sin^4 \theta_2 B_5(t) - \frac{i}{\sqrt{2}}E \cos^2 \theta_2 \sin^2 \theta_2 B_6(t), \\ \dot{B}_6(t) &= -\frac{i}{\sqrt{2}}E \cos^2 \theta_2 \sin^2 \theta_2 B_5(t) - i\frac{1}{2}E \cos^4 \theta_2 B_6(t).\end{aligned}\quad (23)$$

Starting with all initial population in $|D_5(t)\rangle$, Eq. (23) shows that $|D_6(t)\rangle$ is populated when $\cos^2 \theta_2 \sin^2 \theta_2$ is non-vanishing, which is only the case during the turn-on and turn-off of pulses. Choosing small pulse widths therefore assures that effectively all population stays in $|D_5(t)\rangle$ while accumulating the phase. A pulse with FWHM $\tau = 1 \mu\text{s}$ results in the transfer of 0.5% of the population to $|D_6(t)\rangle$ while the smaller FWHM value $\tau = 0.5 \mu\text{s}$ reduces this population to 0.1%. The value $\tau = 0.5 \mu\text{s}$ is experimentally feasible but requires higher Rabi frequencies. Now, in this regime where $B_6(t) \approx 0$, we may readily solve Eq. (23) for $B_5(t)$ and from 19 we obtain:

$$\begin{aligned}\psi_I(t) &= e^{-iE \int_{-\infty}^{t_f} \sin^4 \theta_2 dt}|D_5(t)\rangle \\ &= \cos^2 \theta_2 e^{-iE \int_{-\infty}^{t_f} \sin^4 \theta_2 dt}|11\rangle \\ &\quad - \sin \theta_2 \cos \theta_2 e^{-iE \int_{-\infty}^{t_f} \sin^4 \theta_2 dt}(|12\rangle + |21\rangle) \\ &\quad + \sin^2 \theta_2 e^{-iE \int_{-\infty}^{t_f} \sin^4 \theta_2 dt + iEt}|22\rangle.\end{aligned}\quad (24)$$

Going back to the Schrödinger picture an extra phase associated with the $|22\rangle$ -energy shift is introduced and

$$\begin{aligned}\psi(t) &= e^{-iE|22\rangle\langle 22|t}\psi_I(t) \\ &= e^{-iE \int_{-\infty}^t \sin^4 \theta_2 dt} (\cos^2 \theta_2 |11\rangle \\ &\quad - \sin \theta_2 \cos \theta_2 (|12\rangle + |21\rangle) + \sin^2 \theta_2 |22\rangle).\end{aligned}\quad (25)$$

With all population initially in $|11\rangle$ and application of the STIRAP pulse sequence (2) to both atoms but with only Ω_1 in Fig. 1 applied, we end up in $e^{\gamma_{n_2}}|11\rangle$ after the pulse sequence, where $\gamma_{n_2} = -E \int_{-\infty}^{t_f} \sin^4 \theta_2 dt$. If we, in addition, keep the phases of the laser fields fixed no single-qubit phases are accumulated, i.e.,

$$\begin{aligned}|00\rangle &\rightarrow |00\rangle \\ |01\rangle &\rightarrow |01\rangle \\ |10\rangle &\rightarrow |10\rangle \\ |11\rangle &\rightarrow e^{i\gamma_{n_2}}|11\rangle.\end{aligned}\quad (26)$$

So far, our analysis of the two-qubit gate is general and applicable to various atomic systems such as optically trapped neutral atoms, trapped ions and rare-earth ions doped into crystals. To provide the coupling $E|22\rangle\langle 22|$ we need to be a little more specific, and we suggest in the case of trapped atoms or ions to exploit the long-range dipole-dipole interaction between Rydberg excited atoms [23] and in doped crystals to exploit the interaction between excited states with permanent dipole moments [24]. In [23, 24] the interactions are used for quantum gates in stepwise schemes, where first one atom is excited, and then the interaction blocks the excitation of the second atom, leading to an entanglement between them. This stepwise process is not compatible with our adiabatic protocol, and we suggest instead to apply the interaction to perturb the energy levels of both atoms when their $|2\rangle$ states are coupled off-resonantly to the excited states. As shown in [25], this off-resonant excitation causes an energy shifts (AC Stark shifts) of the $|2\rangle$ states, and due to the dipole-dipole interaction, this shift will have a non-separable component of precisely the desired form for suitable choices of the laser detunings and strengths. The energy shift E is given by a fourth order expansion in Rabi frequencies with a product of three detunings in the denominator, and the gate thus requires relatively long interaction times to avoid population transfer to the excited states.

VI. CONCLUSIONS

We have shown that in the adiabatic limit population transfer in tripod systems introduces purely geometric phases. These phases can be used in quantum information science to form a set of robust geometric gates. The performance of the three gates (1) depends on the robustness of the phases: $\gamma_{n_1} = -\int_{\varphi_i}^{\varphi_f} \sin^2 \theta d\varphi$,

$\gamma_{n_H} = - \int_{\varphi_{H_i}}^{\varphi_{H_f}} \sin^2 \theta_H d\varphi_H$ and $\gamma_{n_2} = -E \int_{-\infty}^{t_f} \sin^4 \theta_2 dt$. The population transfers are done without ever populating the upper state $|e\rangle$ in the tripod system (see Fig. 1), which ensures that the gates are insensitive to spontaneous emission. Pulse shapes, delay between sequences and ratio between Rabi frequencies are routinely controlled experimentally without drift in the laboratory. If we assume systems where the three laser frequencies lie so close that all fields can be generated from the same source, the relative phases of the fields are also easily controllable. This could be achieved when $\{|0\rangle, |1\rangle, |2\rangle\}$

are atomic Zeeman- or hyperfine-substates. In this case all gates are very robust with respect to parameter fluctuations and can be implementable in present-day laboratories.

Acknowledgments

This work is supported by the Danish Research Agency (Grant. No. 2117-05-0081).

[1] D. Deutsch, Proc. R. Soc. London, Ser. A **425**, 73 (1989).
 [2] A. Barenco, C. H. Bennett, R. Cleve, D. P. Divincenzo, N. Margolus, P. Shor, T. Sleator, J. A. Smolin, and H. Weinfurter, Phys. Rev. A **52**, 3457 (1995).
 [3] A. Messiah, *Quantum Mechanics*, vol. 2 (North-Holland publishing company, 1961).
 [4] M. V. Berry, Proc. R. Soc. London, Ser. A **392**, 45 (1984).
 [5] F. Wilczek and A. Zee, Phys. Rev. Lett. **52**, 2111 (1984).
 [6] Y. Aharonov and J. Anandan, Phys. Rev. Lett. **58**, 1593 (1987).
 [7] P. Zanardi and M. Rasetti, Phys. Lett. A **264**, 94 (1999).
 [8] J. A. Jones, V. Vedral, A. Ekert, G. Castagnoli, Nature **403**, 869 (2000).
 [9] A. Recati, T. Calarco, P. Zanardi, J. I. Cirac, and P. Zoller, Phys. Rev. A **66**, 032309 (2002).
 [10] L. M. Duan, J. I. Cirac, and P. Zoller, Science **292**, 1695 (2001).
 [11] K. Bergmann, H. Theuer, and B. W. Shore, Rev. Mod. Phys. **70**, 1003 (1998).
 [12] J. Oreg, F. T. Hioe, and J. H. Eberly, Phys. Rev. A **29**, 690 (1984).
 [13] U. Gaubatz, P. Rudecki, S. Schiemann, and K. Bergmann, J. Chem. Phys. **92**, 5363 (1990).
 [14] B. Broers, H. B. van Linden van den Heuvell, and L. D. Noordam, Phys. Rev. Lett. **69**, 2062 (1992).
 [15] L. S. Goldner, C. Gerz, R. J. C. Spreeuw, S. L. Rolston, C. I. Westbrook, W. D. Phillips, P. Marte, and P. Zoller, Phys. Rev. Lett. **72**, 997 (1994).
 [16] J. Lawall and M. Prentiss, Phys. Rev. Lett. **72**, 993 (1994).
 [17] T. Cubel, B. K. Teo, V. S. Malinovsky, J. R. Guest, A. Reinhard, B. Knuffman, P. R. Berman, and G. Raithel, Phys. Rev. A **72**, 023405 (2005).
 [18] J. L. Sørensen, D. Møller, T. Iversen, J. B. Thomsen, F. Jensen, P. Staanum, D. Voigt, and M. Drewsen, New J. Phys. **8**, 261 (2006).
 [19] R. G. Unanyan, B. W. Shore, and K. Bergmann, Phys. Rev. A **59**, 2910 (1999).
 [20] Z. Kis and F. Renzoni, Phys. Rev. A **65**, 032318 (2002).
 [21] J. K. Pachos and A. Beige, Phys. Rev. A **69** (2004), 033817.
 [22] S. Dasgupta and D.A. Lidar, arXiv:quant-ph/0612201.
 [23] D. Jaksch, J. I. Cirac, P. Zoller, S. L. Rolston, R. Cote, and M. D. Lukin, Phys. Rev. Lett. **85**, 2208 (2000).
 [24] N. Ohlsson, R. K. Mohan and S. Kröll, Opt. Comm. **201**, 71 (2002).
 [25] I. Bouchoule and K. Mølmer, Phys. Rev. A **65**, 041803 (2002).